



EMPIRICAL FRAGILITY FUNCTIONS FROM RECENT EARTHQUAKES

Pooya SARABANDI¹, Dimitris PACHAKIS², Stephanie KING³, Anne KIREMIDJIAN⁴

SUMMARY

In this paper relationships between building performance and ground motion are developed in the form of damage probability matrices and fragility curves using empirical data from recent earthquakes. Data from the 1994 Northridge, California and the 1999 Chi-Chi, Taiwan earthquakes are aggregated and analyzed in order to develop these relationships. Only those buildings located near free-field strong motion recording stations (and on similar site conditions) were extracted from available databases (SAC and LADiv88 building datasets). Two classes of buildings were extracted from their respective datasets – those within 1000 feet of a recording station and those within 1 km of a recording station. Several ground motion parameters and different building performance measures are considered and damage functions are developed for the parameters of which there were sufficient data. Correlation analyses are performed to identify the parameters that best correlate to each ground motion parameter. Resulting empirical fragility curves are introduced for steel moment frame, concrete frame, concrete shear wall, wood frame and rehabilitated unreinforced masonry buildings. Sample damage functions are presented in the paper to illustrate the results of the analyses.

INTRODUCTION

Motion-damage relationships currently used for earthquake loss estimation purposes are based primarily on models developed from expert opinion, such as ATC-13 [1], or models that combine analytical model results with expert opinion, such as HAZUS99 [2]. In recent years, there have been selected efforts undertaken to remedy the lack of useful building performance empirical data. For example, following the 1994 Northridge earthquake, an effort was made to systematically document the effects of earthquake shaking on structures adjacent to locations of strong ground motion recordings. The ATC-38 project [3] involved the inspection of more than 500 buildings located near (within 1000 feet of) 30 strong motion recording stations. The resulting database of building characteristic and performance documentation, photos, and strong motion recordings provides a wealth of information for developing

¹The J. A. Blume Earthquake Engineering Center, Stanford University, Stanford, CA 94305-4020, USA.
Email: psarabandi@stanford.edu

²The J. A. Blume Earthquake Engineering Center, Stanford University, Stanford, CA 94305-4020, USA.

³Email: dpach@stanford.edu

Weidlinger Associates, Los Altos, CA 94022, USA. Email: king@hart.wai.com

⁴Department of Civil and Environmental Engineering, Stanford University, Stanford, CA 94305-4020, USA. Email: ask@stanford.edu

new motion-damage relationships based on non-proprietary empirical data. A similar dataset was also developed following the 1999 Chi-Chi, Taiwan earthquake by Degenkolb Engineers [4].

The availability of comprehensive empirical data on the performance of buildings in earthquakes is one essential part of developing motion-damage relationships. A second essential part is a clear and systematic method for combining that empirical data with the associated recorded ground motion parameters to produce fragility curves and damage probability matrices that can be used in earthquake loss estimation methodologies, structural studies, and in design code formulation. Examples of published material on fragility curve development include Singhal and Kiremidjian [5], who present a method for developing fragility curves using simulated ground motion parameters with analytically-derived building performance data, and Basoz and Kiremidjian [6], who use documented bridge damage and repair cost data with recorded earthquake motions to develop empirical fragility curves for several classes of highway bridges.

In this paper, we developed motion-damage relationships based on the correlation of observed building performance with measured ground motion parameters. Data used for developing the motion-damage relationships were limited to those buildings for which consistent and complete post-earthquake surveys were done and for which a strong ground motion recording instrument is located close enough so that the recorded motion at the instrument site can be assumed to be that experienced at the building site. Due to this limitation, motion-damage relationships (in the form of fragility curves and damage probability matrices) were developed only for the building types with enough data points to result in a statistically significant sample size. The results of motion-damage relationships presented here are part of the work that has been done for *SMIP03* project by King et al. [7] and [8].

MODEL DEVELOPMENT AND METHODOLOGY

In the model development we first focused on the identification of strong correlation between building performance and measured ground motion parameters. Empirical damage probability matrices were developed for all building performance descriptors and the corresponding ground motion or building demand parameters. Damage probability matrices (*DPMs*) show the conditional probability of being in a discrete damage state or performance level as a function of the input ground motion or building demand level, which can be a discrete value (e.g., *MMI*) or a range of values (e.g., *PGA*). Figure 1 illustrates the procedure for developing the damage probabilities for a given ground motion intensity level. For the areas of strong correlation, fragility curves were developed in the form of lognormal probability distributions. Fragility curves show the conditional probability of being equal to or exceeding a given damage state or performance level as a function of the ground motion or building demand parameter. Final *DPMs* were derived from the fragility functions by discretizing the continuous distributions. Figure 1 illustrates the relationship between *DPMs*, probability distributions, and fragility curves.

Building Performance Data

In order to develop meaningful and useful motion-damage relationships that correlate building performance to recorded ground motion data, the datasets need to satisfy certain criteria. These criteria include: Proximity to free-field ground motion recording-stations, non-proprietary nature of the datasets, sufficient number of data points, consistent building survey information, and no bias with respect to building damage meaning that the database contains information of both damaged and undamaged structures.

We first identified and collected datasets that met the above criteria, which were found to be quite stringent and limiting. Extensive data search efforts were undertaken for appropriate datasets from several

recent significant earthquakes, including the 1989 Loma Prieta, the 1994 Northridge, the 1999 Chi-Chi, and the 2000 Nisqually earthquakes. The following datasets were selected to be included in our database: ATC-38 (ATC, 2000) [3], LADiv88 (Los Angeles Division 88 Standard) [9], SAC (FEMA, 2000) [10], and Chi-Chi – Degenkolb Database on the Performance of Buildings Near Strong-Motion Recording Stations [4].

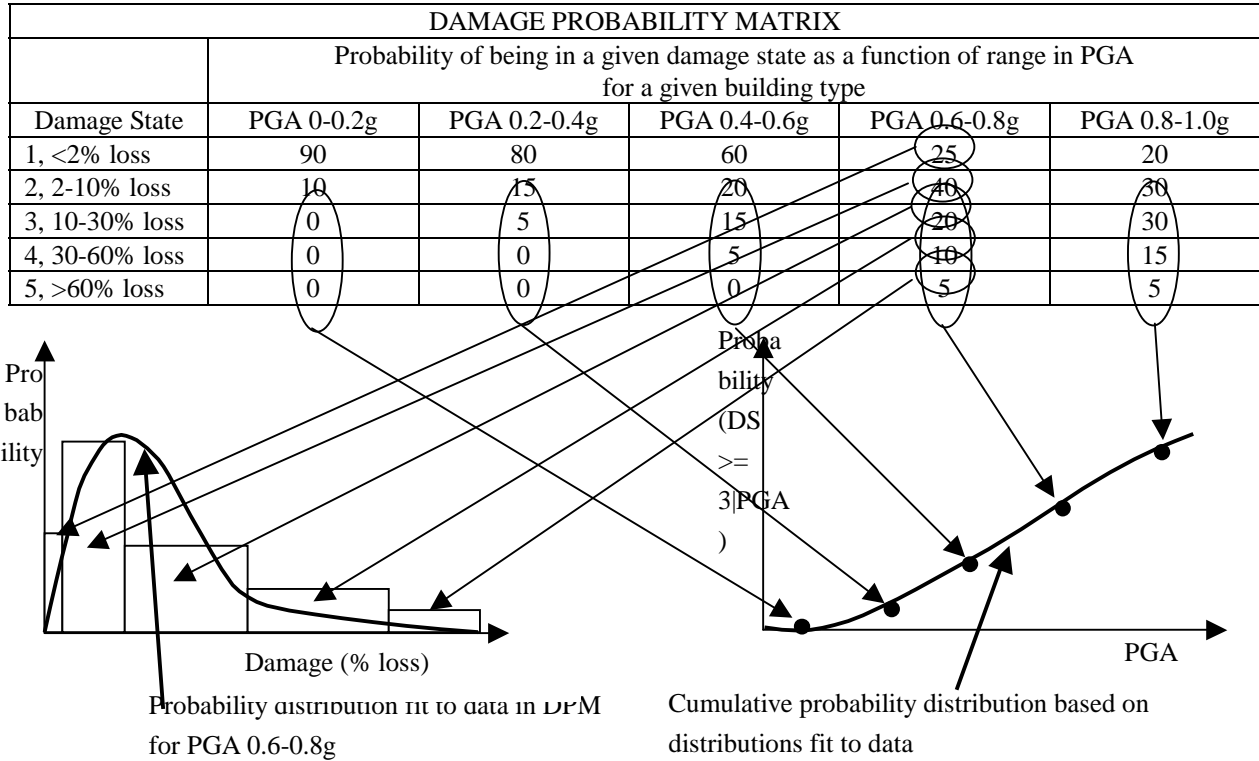


Figure 1. Illustration of relationship among damage probability matrix, probability distribution fit, and fragility curve for hypothetical data.

The buildings in the database were classified according to the FEMA 310 (FEMA, 1998) [11] classification scheme, which is very similar to that used in HAZUS (FEMA, 1999) [2] and several recent ATC projects. Table 1 shows the breakdown of buildings to different classes according to the FEMA 310 [11] model building types.

In addition to a standard classification by structural type, it is necessary to group the buildings by a standard and consistent description of earthquake performance. Four different performance characterizations were used to facilitate more wide-spread use of the developed motion-damage relationships. Table 2 summarizes these four characterizations, namely ATC-13 (ATC, 1985) [1] damage states, HAZUS99 (FEMA, 1999) [2] damage states, FEMA 273/356 (FEMA, 2000) [10] performance levels, and Vision2000 (SEAOC, 1995) [12] performance levels. The performance of each building was described in one of these four characterizations or in terms of percent loss (of building replacement value). A correspondence among the performance characterizations was developed in terms of percent loss as shown in Table 2 so that the performance of each building could be characterized using all four schemes.

Strong Ground Motion Data

Following the collection of the building performance database, the corresponding strong ground motion data were identified and collected by mapping the building locations in a Geographic Information System (GIS) and overlaying a map of the ground motion recording stations. Two classes of buildings were extracted from their respective datasets – those within 1000 feet of a recording station and those within 1 km of a recording station. The 1 km distance criterion was added in order to study the sensitivity of the motion-damage correlations to distance between buildings and recording stations could be done.

Table 1. Summary of Building Performance Data

Model Building Type	Source of Data	Number of Building Records by HAZUS99 Damage State						Total
		Within 1000 feet of Recording Station ¹						
		N ²	S ³	M ⁴	E ⁵	C ⁶	U ⁷	
W1	ATC-38	195	8	6	5	0	21	235
W2	ATC-38	31	2	2	0	0	0	35
S1	SAC, ATC-38	18	6	16	0	0	3	43
S2	ATC-38	5	1	0	1	0	0	7
S3	ATC-38	10	0	0	0	0	0	10
S4	ATC-38	1	0	1	0	0	0	2
S5	ATC-38	6	0	1	0	0	0	7
C1	ATC-38	13	4	2	1	0	0	20
C2	ATC-38, Chi-Chi	48	11	3	0	0	1	63
C3	ATC-38, Chi-Chi	40	22	12	14	0	2	90
PC1	ATC-38	4	6	0	0	0	0	10
PC2	ATC-38	0	0	0	0	0	0	0
RM1	ATC-38	31	32	3	0	0	0	66
RM2	ATC-38	7	9	6	0	1	0	23
URM	ATC-38	2	10	5	0	1	0	18
URM (rehab.)	LADiv88	29	14	10	1	0	0	54
TOTALS		440	125	67	22	2	27	683

¹ Includes both free field and basement level recordings

²None ³Slight ⁴Moderate ⁵Extensive ⁶Complete ⁷Unknown

For the ATC-38 [3] and Chi-Chi building datasets [4], the strong ground motion data are included as database tables linked via the attribute containing the building identification number. All buildings in these two datasets could be used in the analysis as they are all located very close (within 1000 feet) to the recording stations. For the SAC [10] and LADiv88 [9] building datasets, only those buildings located near to free-field strong motion recording stations (and on similar site conditions) could be used.

The final datasets included four basic groups of buildings: the steel, concrete and wood-frame buildings that experienced the Northridge earthquake, and the concrete-frame buildings that experienced the Chi-Chi earthquake. Each building was matched with the corresponding free field or reference strong

ground motion recording station within 1000 feet. Buildings located within 1000 feet of only a basement level recording station were also included, but noted accordingly. In addition, buildings with recording stations located at a distance greater than 1000 feet, but less than 1 km, were also included and so noted.

The strong ground motion parameters, the building response measures, and the building damage states or performance levels were merged in the same database. Table 3 shows those parameters that have been calculated for each building in the database.

Table 2. Correspondence Among Damage States and Percent Loss

ATC-13		HAZUS99	
	% Loss		% Loss
1-None	0	1-None	0-2
2-Slight	0-1		
3-Light	1-10	2-Slight	2-10
4-Moderate	10-30	3-Moderate	10-50
5-Heavy	30-60	4-Extensive	50-100
6-Major	60-100		
7-Destroyed	100	5-Complete	100

FEMA273		Vision2000	
	% Loss		% Loss
1-Very Light	0-1	9,10-Negligible	0-2
2-Light	1-10	7,8-Light	2-10
3-Moderate	10-30	5,6-Moderate	10-50
4-Severe	30-100	3,4-Severe	50-100
		1,2-Complete	100

Table 3. Strong Ground Motion and Building Demand Parameters Used in Project

Intensity or Demand measures (IM)	Symbol	Units
90% Duration	T_{90}	[sec]
Acceleration Spectrum Intensity	ASI	[g]
Arias Intensity	I	[cm/sec]
Bracketed Duration	T_b	[sec]
Effective Peak Acceleration	EPA	[g]
Effective Peak Velocity	EPV	[cm/sec]
Housner Intensity (5% damping)	I_H	[cm/sec]
Maximum Interstory Drift Ratio	IDR_{max}	%
Modified Mercalli Intensity	MMI	-
Peak Ground Acceleration	PGA	[g]
Peak Ground Displacement	PGD	[cm]
Peak Ground Velocity	PGV	[cm/sec]
RMS – total duration	RMS_t	[g]
RMS Acceleration 90%	RMS_{90}	[g]
RMS Bracketed Acceleration	RMS_b	[g]
Shake Map Instrumental Intensity	I_{mm}	-
Spectral Acceleration	S_a	[g]
Spectral Acceleration - design force coefficient ratio	$S_a DBSC$	-
Spectral Displacement	S_d	[cm]
Spectral Roof Drift Ratio	$u_{roof}(\delta_R)$	%
Spectral Velocity	S_v	[cm/sec]
Total Record Duration	T_t	[sec]

Empirical Damage Probability Matrices

The entries of the damage probability matrix (*DPM*) for a given building type are defined as the probability of being in a specific damage state or performance level as a function of the given ground motion or building demand parameter. To calculate the empirical *DPMs*, the building samples were segregated into five bins by partitioning the ranges in ground motion or building demand parameters. For the buildings in each subgroup the empirical distribution of the corresponding damage states or performance levels was calculated. The only exceptions to the partitioning of the ground motion parameters into five bins were the Modified Mercalli Intensity (*MMI*) and the ShakeMap Instrumental Intensity (I_{MM}) that were partitioned in seven ($MMI = VI$ to XII) in order to be consistent with the *MMI* scale and the ATC-13 [1] damage probability matrices.

Fragility Functions

The fragility functions were developed according to the methodology outlined in Singhal and Kiremidjian [5], consisting of the following steps:

1. Isolate from the database the pairs of damage state/performance level and ground motion parameters for all the buildings of a particular building type. The set of all these pairs constitutes the sample to be analyzed.
2. Divide the range of ground motion or building demand parameters into bins. The number of bins to be used depends on the size of the sample, according to one of the typical algorithms used for creating histograms. There should be enough samples in each bin to allow proper fitting of a probability distribution.
3. Use the samples in each bin to fit a lognormal distribution to the data for damage states/performance levels (DS) given the range of the ground motion measure (IM). In other words estimate the parameters of:

$$f_{DS|IM} = \frac{dP[DS \leq ds | IM = im]}{dDS} \quad (1)$$

where im is the midpoint of the bin. The estimation is done by the standard maximum likelihood estimators and a Kolmogorov-Smirnov test is used to determine the goodness of fit.

4. For each bin, the probability of a building being in or exceeding a particular damage state is calculated using the estimated parameters, i.e.

$$P[DS = ds | IM = im], ds = 1, \dots, N_{ds},$$

where N_{ds} is the total number of damage states.

5. Using the probabilities computed in Step 4, a lognormal cumulative distribution function (CDF) is fit to all the points that correspond to the same damage state but different ground motion measures. This fit is accomplished by minimizing the square error. This lognormal CDF is the fragility function and expresses the probability of being in or exceeding a particular damage state as a function of the intensity measure.

The probability of being in, or exceeding, a particular damage state, ds , given the spectral displacement, S_d , is defined in HAZUS99 [2] by the function:

$$P[ds | S_d] = \Phi \left[\frac{1}{\beta_{ds}} \ln \left(\frac{S_d}{\bar{S}_{d,ds}} \right) \right] \quad (2)$$

where:

$\bar{S}_{d,ds}$ is the median value of spectral displacement at which the building reaches the threshold of damage state, ds

β_{ds} is the standard deviation of the natural logarithm of spectral displacement for damage state, ds

Φ is the standard normal cumulative distribution function

The parameters that are estimated from Step 5 correspond to the parameters μ (mean of logarithms) and σ (standard deviation of logarithms) of a lognormal random variable. Thus the correspondence between the two sets of parameters is:

$$\ln \bar{S}_{d,ds} = \mu \rightarrow \bar{S}_{d,ds} = e^\mu \quad (3)$$

$$\beta_{ds} = \sigma \quad (4)$$

Derivation of Damage Probability Matrices

With the parameters of the fragility function, one can easily develop the damage probability matrix, showing the probability of the building being in damage state ds for a given value (or range of values) of the ground motion measure im . For example, using the values of the mid-points of the ground motion intensity measures, the elements of the damage probability matrix, $DPM(i,j)$, are computed as:

$$DPM(i,j) = P[DS = i | IM = im(j)] = P[DS \geq i | IM = im(j)] - P[DS \geq i+1 | IM = im(j)] \quad (5)$$

where:

$im(j)$ is the value of the ground motion measure at the mid-point of the j th bin
 $i = 2, 3, \dots, N_{ds}$; for $i = 1$ the elements are written as:

$$DPM(1,j) = 1 - P[DS \geq 2 | IM = im(j)] \quad (6)$$

Formulation of the fragility functions and $DPMs$ for the Vision2000 [12] performance levels required a slightly modified approach. As can be seen in Table 2, the damage states or performance levels of Vision2000[12] are decreasing from ten to one with increasing damage, in contrast to all other performance levels. For consistency with the fragilities functions and $DPMs$ developed for the other performance levels (ATC-13 [1], FEMA273 [10], and HAZUS99 [2]), it was decided to consolidate the performance levels into five groups of two so that there would be a direct correspondence with the HAZUS99 [2] performance levels. Thus for the fragility function estimation, the probability of a building being in or exceeding a particular damage state (i.e., sustaining heavier damage) is computed from the revised formula as follows:

$$P[DS \leq ds | IM = im], ds = 1, \dots, N_{ds} \quad (7)$$

The elements of the DPM are computed as follows:

$$DPM(1,j) = P[DS = 1 \text{ or } 2 | IM = im(j)] = P[DS \leq 3 | IM = im(j)] - P[DS \leq 1 | IM = im(j)] \quad (8)$$

$$DPM(2,j) = P[DS = 3 \text{ or } 4 | IM = im(j)] = P[DS \leq 5 | IM = im(j)] - P[DS \leq 3 | IM = im(j)] \quad (9)$$

$$DPM(3,j) = P[DS = 5 \text{ or } 6 | IM = im(j)] = P[DS \leq 7 | IM = im(j)] - P[DS \leq 5 | IM = im(j)] \quad (10)$$

$$DPM(4,j) = P[DS = 7 \text{ or } 8 | IM = im(j)] = P[DS \leq 9 | IM = im(j)] - P[DS \leq 7 | IM = im(j)] \quad (11)$$

$$DPM(5,j) = P[DS = 9 \text{ or } 10 | IM = im(j)] = 1 - P[DS \leq 9 | IM = im(j)] \quad (12)$$

RESULTS

For each building class - wood frame, steel frame, and concrete frame buildings- correlations between building performance and measured ground motion parameters are calculated. Furthermore, the concrete frame buildings were separated into those that experienced shaking in the 1994 Northridge earthquake and those that experienced the 1999 Chi-Chi earthquake. This was done because it was decided that although they could be grouped in similar buildings classes, the differences in construction between the two countries were too great. Motion-damage relationships for steel structures were previously presented by the authors [13]. A comparison between motion-damage relationships and commonly-used fragility functions and damage probability matrices for concrete buildings subjected to the 1994 Northridge earthquake is presented in this paper. A complete set of motion-damage relationships for wood frame, steel frame and concrete frame buildings are also presented by King et al. [7] and [8].

Concrete Frame Buildings – Northridge Earthquake

The dataset of concrete frame buildings (Northridge earthquake) includes two classes; C1 (concrete moment resisting frame) and C2 (concrete frame with concrete shear wall), with 20 and 60 buildings, respectively. The correlations of building performance with the ground motion measures are shown in Tables 4 and 5 for class C1 and in Tables 6 and 7 for class C2. Tables 4 and 6 show the correlation for building performance in terms of damage states and performance levels, while Tables 5 and 7 show the correlation for building performance in terms of percent loss. Correlations were also developed for class C3 (concrete frame with masonry in-fill shear wall), but due to the size of the dataset (13 buildings) buildings in this class were not further analyzed.

As can be seen in Tables 4 and 5, the ground motion measures that have the highest correlations to damage are the ASI , EPA , RMS_b , RMS_{90} , PGA , and AI . These tables show that spectral displacement (S_d), spectral acceleration (S_a), and S_aDBSC all appear to be poorly correlated with the performance levels for building class C1, possibly indicating that either the fundamental period of the building changes due to concrete cracking, or the original estimate of the fundamental period is not correct. It should also be noted that significantly higher correlations are obtained for all parameters with percent loss (Table 5) than damage state or performance level (Table 4). The similarity of the correlation values of the HAZUS99 [2] damage states and FEMA 273/356 [10] and Vision2000 [12] performance levels in Table 4 is due to the fact that the same buildings are included in the first three damage states. The correlation values of Vision2000 [12] are negative because the performance levels decrease with increased damage.

As shown in Tables 6 and 7, the correlations for class C2 are quite low, especially in comparison to class C1 correlations shown in Tables 4 and 5. Although the material types (concrete frame) are similar, the lateral load resisting systems significantly influence the observed earthquake performance as predicted from a measured ground motion parameter. The difference could also be due to the disparity in the sample sizes (20 for class C1 and 60 for class C2). The ground motion measures that show relatively higher correlation for C2 buildings are spectral displacement (S_d), I_{MM} , and IDR_{max} . Note that T_b and T_{90} have relatively high negative correlation with damage state or performance level and percent loss, and that lower correlations are obtained for all parameters with percent loss (Table 7) than damage state or performance level (Table 6).

Fragility functions were developed for the C1 and C2 classes for the following ground motion measures that exhibited higher correlation with building performance: S_d (average horizontal), S_d (maximum horizontal), MMI , I_{MM} , EPV , IDR_{max} , δ_R , PGV , S_v , RMS , HI , PGD , S_a , PGA and T_b . Average horizontal values were used for all ground motion measures except spectral displacement. The data are too sparse to enable estimation of fragility parameters for different heights and design code dates, thus the data are combined for all heights resulting in one set of fragility parameters for this building class. The functions were developed for all four standards of building performance (i.e., ATC-13 [1], HAZUS99 [2], FEMA 273/356 [10], and Vision2000 [12]). However, convergence at Step 5 of the procedure outlined earlier in this paper (minimization of the square errors) could not always be achieved. Different initial values were tried for each curve.

The HAZUS99 [2] fragility parameters and the fragility parameters computed (using average horizontal spectral displacement) for the C1 and C2 building classes are shown in Tables 8 and 10, respectively. Note that convergence could not be achieved for the slight and moderate damage states for the C2 buildings in Table 9. Figure 2 shows the fragility curves corresponding to the parameters listed in Table 8, for the high code high-rise C1H buildings from HAZUS99 [2] and as computed in this project for C1 buildings. For all curves, the data sets were small, thus the parameters should be used with caution. For larger values of S_d , the fragility curves for the different damage states do not cross as they do for the

wood and steel frame buildings (not presented in this paper); however, they appear to converge at a probability level of approximately 0.70. The data are concentrated at low S_d values, thus the curves should not be used beyond the S_d range indicated in Figure 2.

Table 4. Correlations Between Ground Motion and Building Demand for Building Class C1

Parameter	ATC 13	FEMA 273/356	HAZUS 99	Vision 2000
ASI	0.676	0.660	0.660	-0.660
EPA	0.671	0.663	0.663	-0.663
RMS _b	0.639	0.585	0.585	-0.585
RMS ₉₀	0.604	0.588	0.588	-0.588
PGA	0.579	0.544	0.544	-0.544
AI	0.575	0.567	0.567	-0.567
I _{MM}	0.566	0.475	0.475	-0.475
PGV	0.551	0.473	0.473	-0.473
RMS	0.545	0.540	0.540	-0.540
? _R	0.520	0.522	0.522	-0.522
EPV	0.510	0.517	0.517	-0.517
HI	0.497	0.485	0.485	-0.485
PGD	0.454	0.387	0.387	-0.387
IDR _{max}	0.377	0.377	0.377	-0.377
MMI	0.343	0.251	0.251	-0.251
Duration	0.296	0.195	0.195	-0.195
S _v	0.276	0.214	0.214	-0.214
T _b	0.157	0.247	0.247	-0.247
S _d	0.063	0.025	0.025	-0.025
S _a	-0.098	-0.159	-0.159	0.159
S _a DBSC	-0.136	-0.214	-0.214	0.214
T ₉₀	-0.383	-0.424	-0.424	0.424

Table 5. Correlations Between Ground Motion and Building Demand Parameters and Percent Loss for Building Class C1

ATC 13	FEMA 273/356	HAZUS 99	Vision 2000
0.747	0.744	0.750	0.750
0.733	0.725	0.732	0.732
0.694	0.708	0.709	0.709
0.670	0.667	0.673	0.673
0.652	0.658	0.664	0.664
0.635	0.617	0.629	0.629
0.615	0.632	0.626	0.626
0.608	0.602	0.607	0.607
0.559	0.559	0.554	0.554
0.532	0.527	0.530	0.530
0.519	0.510	0.512	0.512
0.495	0.481	0.481	0.481
0.438	0.474	0.443	0.443
0.436	0.426	0.433	0.433
0.432	0.477	0.477	0.477
0.317	0.370	0.332	0.332
0.309	0.284	0.311	0.311
0.155	0.130	0.134	0.134
0.098	0.141	0.112	0.112
-0.120	-0.117	-0.111	-0.111
-0.155	-0.146	-0.141	-0.141
-0.341	-0.325	-0.312	-0.312

As shown in Tables 8 and 10 and Figure 2, the differences in the estimated fragility parameters between the various damage states are small, while the HAZUS99 [2] parameters for the damage states are quite distinct. These results are similar to those observed for the steel and wood frame buildings (not presented in this paper), and the same possible explanation holds – the HAZUS99 [2] fragility curves were estimated based on analysis of one model building of this structural type, while the empirically-derived curves come from many buildings of the same structural type. Hence the performance of the particular building population of the same class is not uniform and for the close values of spectral displacement there are buildings in several damage states.

Figures 3 through 6 show additional lognormal fragility curves developed from the C1 building dataset and Figures 7 and 8 show lognormal fragility curves developed from the C2 building dataset. Figures 3 and 4 show the probability of being in or exceeding ATC-13 [1] damage states as a function of HI and I_{MM} and Figures 5 and 6 show the probability of being in or exceeding Vision2000 [12]

performance levels as a function of RMS and I_{MM} for the C1 building type. Figures 7 and 8 show the probability of being in or exceeding ATC-13 [1] performance levels as a function of I_{MM} and Roof Drift Ratio (δ_R) for the C2 building type.

Table 6. Correlations Between Ground Motion and Building Demand for Building Class C2

Parameter	ATC 13	FEMA 273/356	HAZUS 99	Vision 2000
IDR _{max}	0.313	0.178	0.178	-0.178
S _d	0.268	0.154	0.154	-0.154
S _v	0.244	0.063	0.063	-0.063
I _{MM}	0.231	0.211	0.211	-0.211
δ_R	0.223	0.108	0.108	-0.108
HI	0.192	0.135	0.135	-0.135
PGD	0.179	0.086	0.086	-0.086
PGV	0.159	0.142	0.142	-0.142
MMI	0.103	-0.027	-0.027	0.027
RMS _b	0.096	0.024	0.024	-0.024
Duration	0.061	0.012	0.012	-0.012
RMS ₉₀	0.006	-0.044	-0.044	0.044
EPV	0.005	0.037	0.037	-0.037
S _a DBSC	-0.003	-0.042	-0.042	0.042
EPA	-0.042	-0.090	-0.090	0.090
PGA	-0.057	-0.115	-0.115	0.115
ASI	-0.064	-0.111	-0.111	0.111
S _a	-0.074	-0.139	-0.139	0.139
AI	-0.105	-0.149	-0.149	0.149
RMS	-0.107	-0.090	-0.090	0.090
T ₉₀	-0.350	-0.290	-0.290	0.290
T _b	-0.496	-0.388	-0.388	0.388

Table 5. Correlations Between Ground Motion and Building Demand Parameters and Percent Loss for Building Class C1

ATC 13	FEMA 273/356	HAZUS 99	Vision 2000
0.115	0.098	0.060	0.060
0.123	0.109	0.086	0.086
0.044	0.025	0.008	0.008
0.195	0.189	0.173	0.173
0.042	0.028	-0.007	-0.007
0.129	0.122	0.112	0.112
0.093	0.083	0.078	0.078
0.133	0.129	0.119	0.119
-0.047	-0.060	-0.072	-0.072
0.025	0.018	0.014	0.014
0.061	0.057	0.075	0.075
-0.036	-0.040	-0.037	-0.037
0.025	0.028	0.023	0.023
-0.072	-0.076	-0.088	-0.088
-0.077	-0.080	-0.072	-0.072
-0.094	-0.097	-0.086	-0.086
-0.097	-0.100	-0.092	-0.092
-0.146	-0.150	-0.150	-0.150
-0.125	-0.126	-0.113	-0.113
-0.098	-0.095	-0.094	-0.094
-0.250	-0.239	-0.209	-0.209
-0.328	-0.311	-0.267	-0.267

Damage probability matrices were developed for the same parameters for which the fragility curves were: S_d (average horizontal), S_d (max. [2] horizontal), MMI , I_{MM} , EPV , IDR_{max} , δ_R , PGV , S_v , RMS , HI , PGD , S_a , PGA and T_b . The matrices were developed from the raw empirical data and also derived from the fragility curves. Those derived from the fragility curves are discussed in previous section. Damage probability matrices in terms of Modified Mercalli Intensity (MMI) for the C1 building class can be compared to the DPM s published in ATC-13 [2]. Table 10 shows the comparison of the DPM computed for class C1 with the DPM published in ATC-13 [2] for high-rise concrete moment frame buildings (Class 20).

As shown in Table 10, the two damage probability matrices are quite different. The ATC-13 [2] DPM , developed by fitting Beta distributions to expert opinion data, shows a significant increase in probabilities of being in higher damage states for higher levels of MMI . Although, the empirically derived DPM (derived from the lognormal fragility curves) also shows an increase, it is very gradual. Note that

the empirical data were clustered at lower damage levels, thus the empirically derived *DPM* does not have values for damage states greater than moderate. This reflects a very narrow probability distribution on damage at each *MMI* level that does not realistically portray the expected seismic performance of concrete frame buildings. In addition, most of the empirical data points are at *MMI* levels of IX or lower, thus the probabilities associated with *MMI* X and XI should not be used.

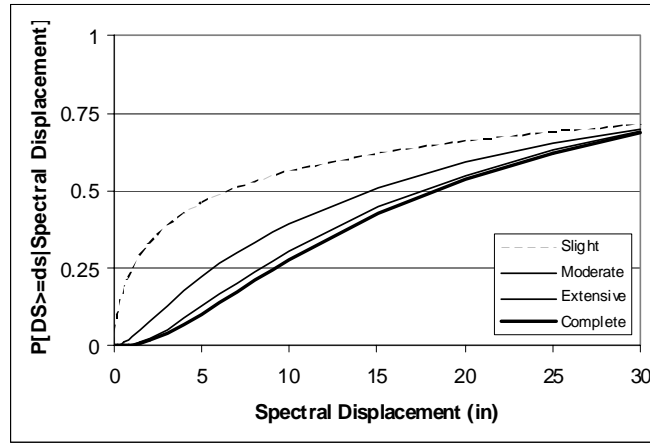
Table 8. Fragility Parameters from HAZUS99 and from Project for Building Class C1 (Northridge Earthquake)

		Median S_a (in) and Lognormal Standard Deviation (Beta)							
Code Level	Bldg. Type	Slight		Moderate		Extensive		Complete	
		Median	Beta	Median	Beta	Median	Beta	Median	Beta
HighCode	C1L	0.90	0.81	1.80	0.84	5.40	0.86	14.4	0.81
	C1M	1.50	0.68	3.00	0.67	9.00	0.68	24.00	0.81
	C1H	2.16	0.66	4.32	0.64	12.96	0.67	34.56	0.78
Moderate Code	C1L	0.90	0.89	1.56	0.90	4.20	0.90	10.8	0.89
	C1M	1.50	0.70	2.60	0.70	7.00	0.70	18.00	0.89
	C1H	2.16	0.66	3.74	0.66	10.08	0.76	25.92	0.91
Low Code	C1L	0.90	0.95	1.44	0.91	3.60	0.85	9.00	0.97
	C1M	1.50	0.70	2.40	0.74	6.00	0.86	15.00	0.98
	C1H	2.16	0.70	3.46	0.81	8.64	0.89	21.60	0.98
Pre-Code	C1L	0.72	0.98	1.15	0.94	2.88	0.90	7.20	0.97
	C1M	1.20	0.73	1.92	0.77	4.80	0.83	12.00	0.98
	C1H	1.73	0.71	2.76	0.8	6.91	0.94	17.28	1.01
HAZUS99	Max.	2.16	0.98	4.32	0.94	12.96	0.94	34.56	1.01
Bounds	Min.	0.72	0.66	1.15	0.64	2.88	0.67	7.20	0.78
Fitted Parameters		6.67	2.71	14.55	1.39	17.42	1.09	18.32	1.02

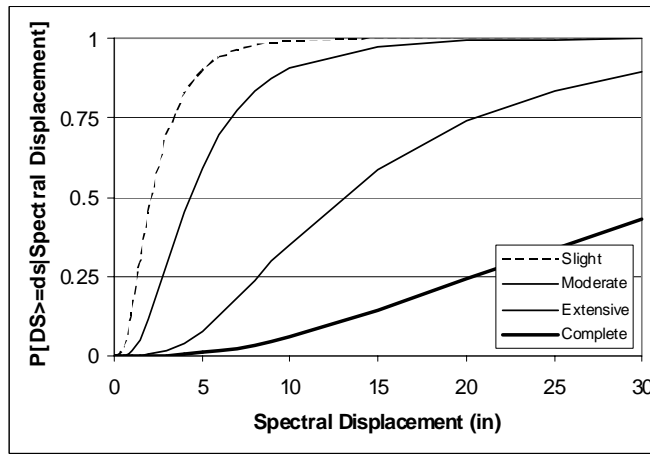
Table 9. Fragility Parameters from HAZUS99 and from Project for Building Class C2 (Northridge Earthquake)

		Median S_a (in) and Lognormal Standard Deviation (Beta)							
Code Level	Bldg. Type	Slight		Moderate		Extensive		Complete	
		Median	Beta	Median	Beta	Median	Beta	Median	Beta
High Code	C1L	0.72	0.81	1.80	0.84	5.40	0.93	14.40	0.92
	C1M	1.20	0.74	3.00	0.77	9.00	0.68	24.00	0.77
	C1H	1.73	0.68	4.32	0.65	12.96	0.66	34.56	0.75
Moderate Code	C1L	0.72	0.91	1.52	0.97	4.17	1.03	10.80	0.87
	C1M	1.20	0.81	2.53	0.77	6.95	0.73	18.00	0.91
	C1H	1.73	0.66	3.64	0.68	10.00	0.70	25.92	0.87
Low Code	C1L	0.72	1.04	1.37	1.02	3.55	0.99	9.00	0.95
	C1M	1.20	0.82	2.29	0.81	5.92	0.81	15.00	0.99
	C1H	1.73	0.68	3.30	0.73	8.53	0.84	21.60	0.95
Pre-Code	C1L	0.58	1.11	1.10	1.09	2.84	1.07	7.20	0.93
	C1M	0.96	0.86	1.83	0.83	4.74	0.80	12.00	0.98
	C1H	1.38	0.73	2.64	0.75	6.82	0.92	17.28	0.97
HAZUS99	Max.	1.73	1.11	4.32	1.09	12.96	1.07	34.56	0.99

Bounds	Min.	0.58	0.66	1.1	0.65	2.84	0.66	7.20	0.75
Fitted Parameters		NA	NA	NA	NA	19.06	0.67	21.50	0.65



(a)



(b)

Figure 2. Fragility curves for C1 building class (Northridge earthquake), (a) computed in the project and (b) from HAZUS99 (class C1H high code).

Table 10 Damage probability matrix for C1 building class (Northridge earthquake), (a) computed and (b) from ATC-13 (class 20, high-rise concrete moment frame).

Damage State	Modified Mercalli Intensity						Damage State	Modified Mercalli Intensity					
	VI	VII	VIII	IX	X	XI		VI	VII	VIII	IX	X	XI
1-None	0.89	0.71	0.48	0.28	0.15	0.07	1-None	~ 0	~ 0	~ 0	~ 0	~ 0	~ 0
2-Slight	0.04	0.16	0.31	0.43	0.47	0.47	2-Slight	0.23	0.02	~ 0	~ 0	~ 0	~ 0
3-Light	0.02	0.05	0.11	0.17	0.23	0.29	3-Light	0.78	0.98	0.83	0.28	0.03	0.01
4-Moderate	0.01	0.02	0.04	0.06	0.08	0.10	4-Moderate	~ 0	~ 0	0.16	0.72	0.85	0.45
5-Heavy	~ 0	~ 0	~ 0	~ 0	~ 0	~ 0	5-Heavy	~ 0	~ 0	~ 0	0.01	0.12	0.54
6-Major	~ 0	~ 0	~ 0	~ 0	~ 0	~ 0	6-Major	~ 0	~ 0	~ 0	~ 0	~ 0	~ 0
7-Destroyed	~ 0	~ 0	~ 0	~ 0	~ 0	~ 0	7-Destroyed	~ 0	~ 0	~ 0	~ 0	~ 0	~ 0

(a)

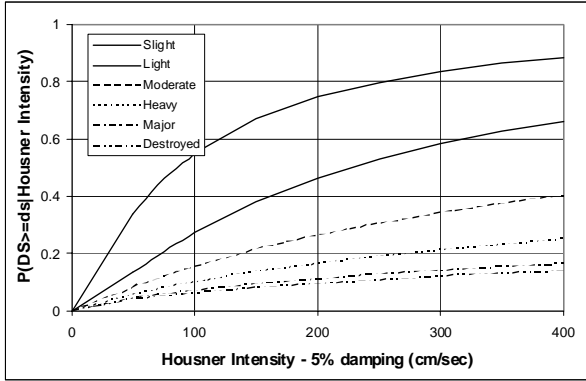


Figure 3. Fragility curves for C1 buildings, ATC-13 damage states, and parameter H_I .

(b)

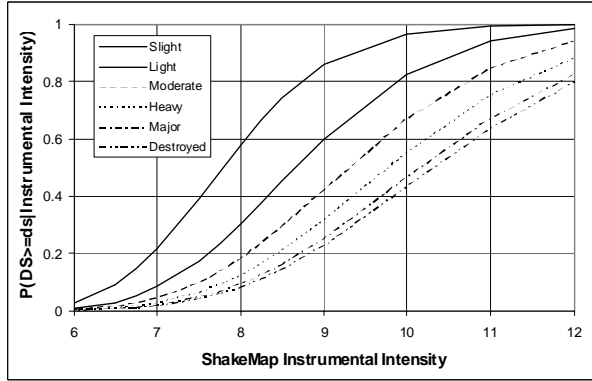


Figure 4. Fragility curve for C1 buildings ATC-13 damage states, and parameter I_{MM} .

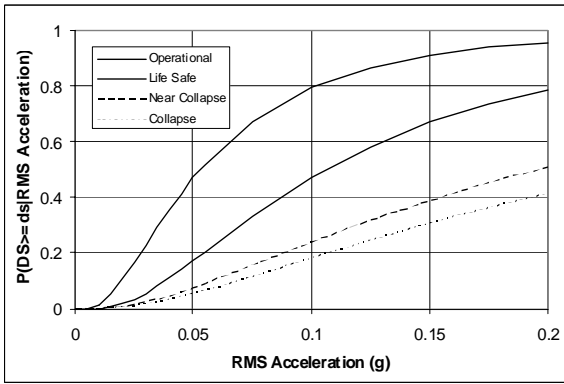


Figure 5. Fragility curves for C1 buildings, Vision2000 performance levels, and parameter RMS .

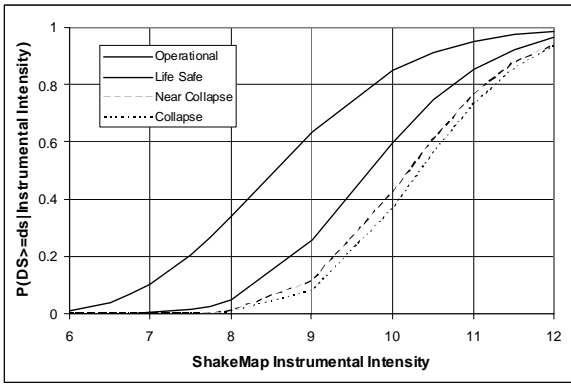


Figure 6. Fragility curve for C1 buildings, Vision2000 performance levels, and parameter I_{MM} .

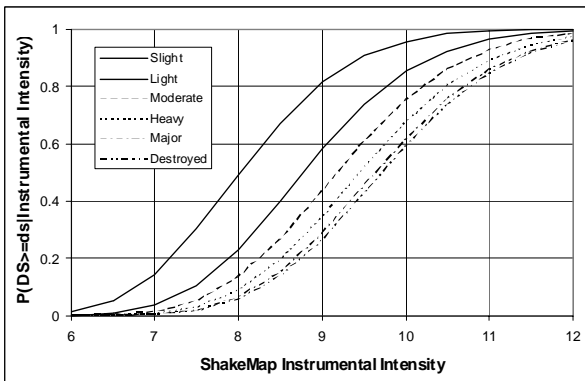


Figure 7. Fragility curve for C2 buildings, ATC-13 damage states, and parameter I_{MM} .

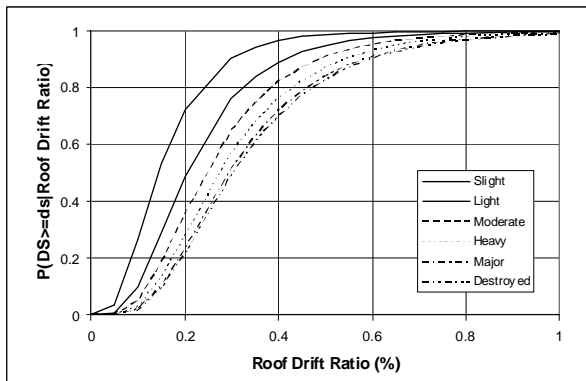


Figure 8. Fragility curve for C2 buildings, ATC-13 damage states, and parameter δ_R .

CONCLUSIONS

The following observations can be made about the results presented in this study keeping in mind that the analysis were based on limited amount of data:

1. A method for developing empirical motion-damage relationships in the form of lognormal fragility curves and derived damage probability matrices was described and illustrated.
2. A database of strong ground motion parameters based on recordings from the 1994 Northridge, California and 1999 Chi-Chi, Taiwan earthquake was developed and is available for use in future research.
3. A database of consistent building performance information with computed seismic demand parameters was developed and is also available for use in future research.
4. Numerous sets of fragility curves for six model building types, including wood, steel, and concrete frame, were developed for several strong ground motion and building demand parameters, based on four different characterizations of building performance.
5. Regional and site-specific earthquake loss estimation applications of the developed motion-damage relationships indicate that although the fragility curves are significantly different from published models, the loss results produced with these relationships are similar to those produced with the published models.
6. A comparison of correlation between building performance and measured strong ground motion using two different site-to-station distances (1000 feet and 1 km) proved inconclusive due to the limited data sample size.
7. Future post-earthquake investigation work should focus on the systematic and accurate gathering and archiving of non-proprietary building performance (including damaged and undamaged structural and nonstructural systems) data near to strong ground motion recording stations, including considerations of: (1) large sample sizes of common model building types, (2) wide range in building performance, and (3) wide range in strong ground motion levels.
8. Data collected in future earthquakes can be added to the datasets developed in this project and the fragility curves can be updated using the methodology outlined in this report.

ACKNOWLEDGMENT

This research was supported by the California Geological Survey (formerly the California Department of Conservation, Division of Mines and Geology), Strong Motion Instrumentation Program (SMIP), contract 1000-743. We express our gratitude to Degenkolb Engineers for providing us with the Chi-Chi, Taiwan data; Rutherford and Chekene Consulting Engineers for providing us with Los Angeles Division 88 database and David Bonowitz for providing us with the SAC Steel Frame Building database.

REFERENCES

1. ATC, 1985, "Earthquake Damage Evaluation Data for California," *ATC-13 Report, Applied Technology Council, Redwood City, CA.*
2. FEMA, 1999, "HAZUS Earthquake Loss Estimation Methodology," *Technical Manual, Prepared by the National Institute of Building Sciences for the Federal Emergency Management Agency, Washington, DC.*

3. ATC, 2000, "Database on the Performance of Structures Near Strong-Motion Recordings: 1994 Northridge, California, Earthquake," *ATC-38 Report, Applied Technology Council, Redwood City, CA.*
4. Heintz, J.A. and Poland, C.D., 2001, "Correlating Measured Ground Motion with Observed Damage," *Earthquake Spectra*, Supplement A to Volume 17, pp. 110-130.
5. Singhal, A. and Kiremidjian, A.S., 1996, *A Method for Earthquake Motion-Damage Relationships with Application to Reinforced Concrete Frames*, John A. Blume Earthquake Engineering Center, Technical Report No. 119, Stanford University, Stanford, CA
6. Basoz, N. and Kiremidjian, A.S., 1999, "Development of Empirical Fragility Curves for Bridges," *Optimizing Post-Earthquake Lifeline System Reliability*, Technical Council on Lifeline Earthquake Engineering Monograph No. 16, Proceedings of the 5th U.S. Conference on Lifeline Earthquake Engineering, American Society of Civil Engineers, Reston, Virginia, pp 693-702.
7. King, S.A., A.S. Kiremidjian, P. Sarabandi, and D. Pachakis, 2003, "Correlation of Observed Building Performance with Measured Ground Motion," Proceedings of the SMIP03 Seminar on Utilization of Strong Motion Data, California Geological Survey, California Department of Conservation, Sacramento, California.
8. King, S.A., A.S. Kiremidjian, P. Sarabandi, and D. Pachakis, 2003, "Correlation of Observed Building Performance with Measured Ground Motion," *Final Project Report (in review)*, California Geological Survey, California Department of Conservation, Sacramento, California.
9. Lizundia, B. and Holmes, W.T., 1997, "The performance of rehabilitated URM buildings in the Northridge earthquake," *Proceedings of the NEHRP Conference and Workshop on Research on the Northridge, California Earthquake of January 17, 1994*, California Universities for Research in Earthquake Engineering (CUREe), Richmond, California, Vol. III-A, 1998, pages III-116 - III-123.
10. FEMA, 2000, "*Recommended Seismic Evaluation and Upgrade Criteria for Existing Welded Steel Moment-Frame Buildings*," Report FEMA-351, Prepared by the SAC Joint Venture for the Federal Emergency Management Agency, Washington, DC.2000.
11. FEMA, 1998, "*Handbook for the Seismic Evaluation of Buildings – A Prestandard*," Report FEMA 310, Prepared by the American Society of Civil Engineers for the Federal Emergency Management Agency, Washington, DC. 2000.
12. SEAOC, 1995, "Performance based seismic engineering of buildings (Vision2000)," *Structural Engineers Association of California*," Sacramento, CA.
13. P. Sarabandi, D. Pachakis, A.S. Kiremidjian and S. King, "Development of Empirical Building Performance Functions Data from Past Earthquakes", *Proceedings of ICASP-9*, July 2003, San Francisco, CA, pp.629-635.